Indian Journal of Chemistry
Vol. 59A, October 2020, pp. 1449-1456

Crystal structure, Hirshfeld surface analysis, DFT and TD-DFT studies of nickel(II) monohydrate complex coordinated by bis (5-bromo-1-formylphenolate) moiety and two water molecules

I Rama*, A Subashini & R Selvameena

PG and Research Department of Chemistry, SeethalakshmiRamaswami College (Autonomous), Affiliated to Bharathidasan University, Tiruchirappalli 620 002, Tamil Nadu, India
Email: rama14jai@yahoo.co.in

Received 20 May 2019; revised and accepted 15 June 2020

In the title compound $[Ni(C_7H_5O_2Br)_2(H_2O)_2]H_2O$, the Ni atom adopts distorted octahedral geometry in which the bidentate ligand acts as O,O' donor defining an equatorial plane and water molecules occupy the axial positions. It is a mononuclear compound. This compound is crystallized on the monoclinic system, space group $P2_1/c$ with the unit cell parameters a = 18.4561(8) Å, b = 7.3442(4) Å, c = 14.5786(8)Å, α= 90°, β= 109.057°, γ = 90° and Z = 4. The two hydroxyl groups are deprotonated and oxygen anions get coordinated with nickel. The supramolecularself-assembly of the complex is also stabilized by weak non-covalent interactions in the crystal packing, which is further quantified by using Hirshfeld surface analysis. The molecular architecture of the complex is examined by quantum chemical calculations using DFT and is compared with crystalline structure of the same. The electronic excitation energies of the complex have been simulated at TD-DFT level and are evaluated with experimental electronic spectrum.

Keywords: Angular distortions, Hirshfeld analysis, HOMO-LUMO energy gap, Molecular electrostatic potential, X-ray diffraction

The design and synthesis of metal-organic scaffolds have involved significant interest as of their potential uses as function materials as well as their structural diversity and intriguing variety of topologies[1–6]. Stable aromatic hydroxyl aldehydes form complexes and the presence of a phenolic hydroxyl group at their o-position reports a supplementary donor site of the molecule making it bidentate. Such a molecule coordinates with the metal ion through the carbonyl oxygen and deprotonated hydroxyl group. The chelating properties of o-hydroxy aldehydes are well established[7]. Hydrogen bonding patterns involved in metal complexes are of current attention[8]. Such interactions can be utilized for designing supramolecular architectures. The crystal structures of five transition metal (Mn, Co, Ni, Cu and Zn) complexes of sulfosalicylate ions have been previously reported in literature[9-13]. The crystal structure of copper complex of Schiff base derived from sulfamethoxazole has been already reported from our laboratory[14].

This paper reports the synthesis and characterization of a mononuclear nickel(II) complex and its structure has been solved by single crystal X-ray crystallography. In order to understand the intermolecular interactions within the crystal structure a powerful technique called Hirshfeld surface analysis is used. This allows easy identification of characteristic interactions throughout the structure and surface around the molecule. Theoretical calculations were performed over the structure of the complex to compare the parameters of the complex in solid and gas phase.

Materials and Methods

The chemicals were purchased from Himedia chemicals used without further purification. Spectroscopic grade solvents were used throughout the experiments.

Synthesis of complex

5-bromo-2-hydroxy benzaldehyde (0.2 g Himedia) and $Ni(CH_3COO)_2.4H_2O$ (0.1244 g Merck) were dissolved separately in hot ethanolic solution mixed in 2:1 molar ratio. The resultant solution obtained was refluxed for half an hour over a water bath and stirred for three hours using a magnetic stirrer. On slow evaporation crystalline material was obtained and further recrystallized using ethanol resulted in fluorescent green crystals of title compound.

X-ray crystallography and refinement

A fluorescent green crystal of dimensions 0.30 ×0.25 ×0.20 mm was taken for X-ray diffraction analysis. The total number of reflections 3881 was collected at room temperature 293(2) K on Bruker AXS SMART CCD[15] diffractometer using graphite monochromated MoK_α radiation. Direct method was used to solve the structure. The structure was refined by full – matrix least squares on F^2. To solve the structure, the programs used were SHELXS-97, SHELXL-97[16] and PLATON[17]. A summary of crystal data and structure refinement is given in Table 1.

All the non-hydrogen atoms were refined anisotropically. The hydrogen atoms of the water molecules were located in difference Fourier map and refined as riding. The other hydrogen atoms were placed in idealized locations and refined as riding. The 5-bromo salicylate anions are found to be disordered over two possible orientations. (We were able to assign two sets of phenyl group with bromine atoms corresponding to the disorder). The occupancy factor refined to 0.766(7) for atoms C3, C4, C5, Br1, C10, C11, C12, Br2 and to 0.234(7) for atoms C3', C4', C5', Br1', C10', C11', C12', Br2'. The uncoordinated water molecule has also disordered with partial occupancy. Hence the hydrogen atoms of water were not located. The anisotropic displacement parameters of atoms C3, C3', Br2 and Br2' were restrained by *DELU* and those of C3 and Br2' were also restrained by *SIMU*. The R value of the title compound is found to 4.

Table 1 — Crystal data and structure refinement for title compound

Molecular formula	$C_{14}H_{12}Br_2NiO_7$
CCDC deposit No.	945220
Formula weight	510.77
Temperature	293(2) K
Wavelength	0.71073 Å
Crystal system	Monoclinic
space group	$P2_1/c$
Unit cell dimensions	
a (Å)	18.4561(8)
b (Å)	7.3442(4)
c (Å)	14.5786(8)
α (°)	90
β (°)	109.057(2)
γ (°)	90
Volume (A^3)	1867.76(17)
Z	4
Density (Calc.) (mg/m^3)	1.816
Absorption coefficient (mm^{-1})	5.347
F(000)	1000
Crystal size (mm)	0.30 x 0.25 x 0.20
θ range for data collection (°)	2.33 - 26.72
Limiting indices	−23:23; −9:9; −16:18;
Max. and min. transmission	0.4144 and 0.2969
Refinement method	Full-matrix least-squares on F^2
Data / restraints / parameters	3881 / 187 / 320
Goodness-of-fit on F^2	1.024
Final R indices [I>2sigma(I)]	R1 = 0.0408, wR2 = 0.1129
R indices (all data)	R1 = 0.0832, wR2 = 0.1336
Extinction coefficient	0.0008(4)
Largest diff. peak and hole (e. $Å^{-3}$)	0.935 and −0.512

Hirshfeld surface analysis

Hirshfeld surfaces (HSs) and 2D fingerprint plots (FPs) were generated using Crystal Explorer 3.1 based on results of single crystal X-ray diffraction studies. The distance from the Hirshfeld surface to the nearest nucleus inside and outside the surface were marked by d_i and d_e, respectively, whereas d_{norm} is a normalized contact distance, which is defined in terms of d_i, d_e and the van der Waals (vdW) radii of the atoms. From the 2D fingerprint plot the existence of different types of intermolecular interactions were recognized.

Computational details

To gain a detailed information regarding the structure of the nickel complex in gaseous state, DFT-B3LYP with 6-31G (d,p) basis set correlation functional calculations have been performed using Gaussian 03W program [18]. The electronic spectrum simulation of the complex was made using time dependent density function theory (TD-DFT)/B3LYP method.

Results and Discussion

The reaction of nickel acetate with 5-bromo-2-hydroxy benzaldehyde in 1:2 molar ratio results in the formation of diaquabis (5-bromo-1-formyl phenolato-k^2O,O') nickel(II) monohydrate. A mixture of ethanol–DMF solution is used to recrystallise the above formed nickel complex. The structure of the complex is confirmed through single crystal X-ray diffraction analysis.

Structure analysis through Single crystal XRD

The nickel complex crystallizes in the monoclinic system with space group $P2_1/c$ (Table 1). The bond distance and angles are listed in Table 2a and 2b. The structure of $[Ni(C_7H_5O_2Br)_2.(H_2O)_2]H_2O$ with atom-labeling as shown in Fig. 1 consists of discrete $[Ni(C_7H_5O_2Br)_2(H_2O)_2]$ and five water molecules at the lattice.

The shortest Ni-O bond length is 2.008(2)Å [Ni(1)-O(4)] and the longest is 2.049(3) Å[O(5)-Ni(1)]. The bond angles ranges from 178.54(12)° [O(6)-Ni(1)-

Table 2 — (a) The selected bond lengths for title compound

Bond length (Å)	XRD	B3LYP6-31G(d,p)	Bond length (Å)	XRD	B3LYP6-31G(d,p)
O(5)-Ni(1)	2.049(3)	3.018	Ni(1)-O(4)	2.008(2)	1.827
Ni(1)-O(2)	2.009(2)	1.85	Ni(1)-O(3)	2.023(3)	1.827
Ni(1)-O(1)	2.025(3)	1.85	O(6)-Ni(1)	2.030(2)	3.017
C(1)-O(4)	1.299(5)	1.264	C(8)-O(2)	1.296(5)	1.29
C(7)-O(1)	1.209(5)	1.29	C(9)-C(10')	1.25(3)	-
C(9)-C(10)	1.414(10)	1.374	C(14)-O(3)	1.224(5)	1.264
C(2)-C(3')	1.32(3)	1.424	C(6)-C(5')	1.46(3)	1.374
C(13)-C(12')	1.29(3)	1.424	C(4)-C(5)	1.355(7)	1.418
C(4)-Br(1)	1.908(6)	1.91	C(11)-Br(2)	1.898(5)	1.91
C(3')-C(4')	1.354(10)	1.369	C(4')-C(5')	1.355(10)	-
C(4')-Br(1')	1.908(9)	-	C(10')-C(11')	1.369(10)	1.418
C(11')-C(12')	1.339(10)	1.369	C(11')-Br(2')	1.900(9)	-

(b)The selected bond angles for title compound

Bond length (°)	XRD	B3LYP	Bond angle6-31G(d,p)	XRD (°)	B3LYP6-31G(d,p)
O(4)-Ni(1)-O(2)	176.80(10)	177.38	O(4)-Ni(1)-O(3)	85.78	88.13(10)
O(2)-Ni(1)-O(3)	91.58(11)	94.53	O(4)-Ni(1)-O(1)	94.51	92.07(10)
O(2)-Ni(1)-O(1)	88.49(10)	85.3	O(3)-Ni(1)-O(1)	177.39	175.15(12)
O(4)-Ni(1)-O(6)	87.47(10)	102.27	O(2)-Ni(1)-O(6)	75.16	89.38(11)
O(3)-Ni(1)-O(6)	93.76(13)	108.66	O(1)-Ni(1)-O(6)	73.83	91.09(13)
O(4)-Ni(1)-O(5)	92.15(11)	108.38	O(2)-Ni(1)-O(5)	74.1	91.02(11)
O(3)-Ni(1)-O(5)	87.63(13)	102.29	O(1)-Ni(1)-O(5)	75.15	87.51(12)
O(6)-Ni(1)-O(5)	178.54(12)	137.56	O(4)-C(1)-C(6)	124.15	124.2(3)
O(4)-C(1)-C(2)	119.6(3)	118.83	O(2)-C(8)-C(9)	126.41	119.8(3)
O(2)-C(8)-C(13)	124.4(3)	126.41	O(1)-C(7)-C(6)	126.41	128.7(4)
C(10')-C(9)-C(8)	123(2)	121.23	O(3)-C(14)-C(13)	118.83	129.1(4)
C(7)-O(1)-Ni(1)	124.2(3)	126.36	C(14)-O(3)-Ni(1)	127.42	123.0(3)
C(1)-O(4)-Ni(1)	125.4(2)	126.36	C(8)-O(2)-Ni(1)	126.37	125.3(2)
C(3')-C(2)-C(1)	118(2)	119.41	C(1)-C(6)-C(5')	121.23	121.8(17)
C(7)-C(6)-C(5')	112.3(17)	121.23	C(12')-C(13)-C(8)	120.63	118(2)
C(12')-C(13)-C(14)	117(2)	119.41	C(12')-C(11')-C(10')	120.33	120.4(12)
C(4)-C(3)-C(2)	118.7(9)	119.97	C(12')-C(11')-C(10')	120.4(12)	-
C(5)-C(4)-Br(1)	119.3(5)	119.03	C(3)-C(4)-Br(1)	120.64	119.7(5)
C(4)-C(5)-C(6)	121.8(9)	120.82	C(12)-C(11)-Br(2)	120.64	120.2(5)
C(10)-C(11)-Br(2)	118.9(5)	120.64	C(13)-C(12')-C(11')	119.97	122(4)
C(2)-C(3')-C(4')	125(3)	-	C(10')-C(11')-Br(2')	119.03	119.0(11)
C(5')-C(4')-C(3')	121.3(12)	120.33	C(3')-C(4')-Br(1')	120.64	119.5(11)
C(4')-C(5')-C(6)	114(3)	120.82	C(4')-C(5')-C(6)	120.82	114(3)
C(9)-C(10')-C(11')	119(4)	120.82	C(12')-C(11')-Br(2')	120.6(11)	-

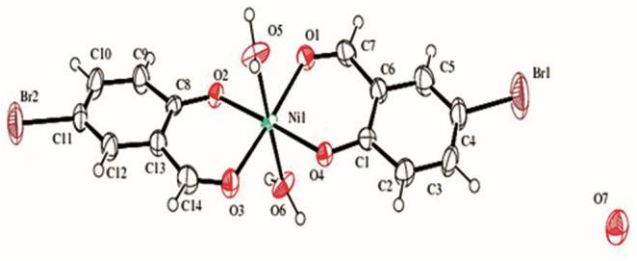

Fig. 1 — ORTEP view of the nickel complex.

O(5)] to 175.15(12)° [O(3)-Ni(1)-O(1)] and from 87.47(10)° [O(4)-Ni(1)-O(6)] to 93.76(13)° [O(3)-Ni(1)-O(6)]. The six coordination sites are occupied by O, O' donor set of two ligands and two water molecules. The two hydroxyl groups are deprotonated and oxygen anions get coordinated with nickel. The value of the transoid angle is 178.54(12)° [O(6)-Ni(1)-O(5)] and slightly deviate from the ideal value of 180° while the cisoid angles have the values in the range 87.47(10)° [O(4)-Ni(1)-O(6)] to 93.76(13)° [O(3)-Ni(1)-O(6)]. These values show that, Ni(II) exhibits distorted octahedral geometry[19].

Hydrogen bonding

The lattice becomes stable by relatively strong hydrogen bonds between the coordinated water oxygens and 5-bromo salicylate anions through O–H…O hydrogen bonds. One of the coordinated

water hydrogen (O5-H5B) acts as a bifurcated donor to two oxygen atoms of two different 5-bromo salicylate anions (O1 & O2) forming a ring with graph – set notation $R^1_2(4)$. Another hydrogen (H5A) atom interacts with $O4^i$ atom through O–H…O hydrogen bond. O6 coordinated water molecule acts as a donor and two different 5-bromo salicylate anions ($O4^{iii}$& $O2^{iv}$) through O–H…O hydrogen bonds. A diagram showing this network is in Fig. 2. The hydrogen bonding patterns between the ligands and water molecules are listed in the Table 3. A three dimensional overall packing interaction is shown in Fig. 3.

Hirshfeld surface analysis

In order to determine the various molecular interactions, Hirshfeld surface and its associated 2D finger print plots were calculated using crystal explorer[20] 3.1. The Hirshfeld surface of the title compound is illustrated in the Fig. 4 showing surfaces

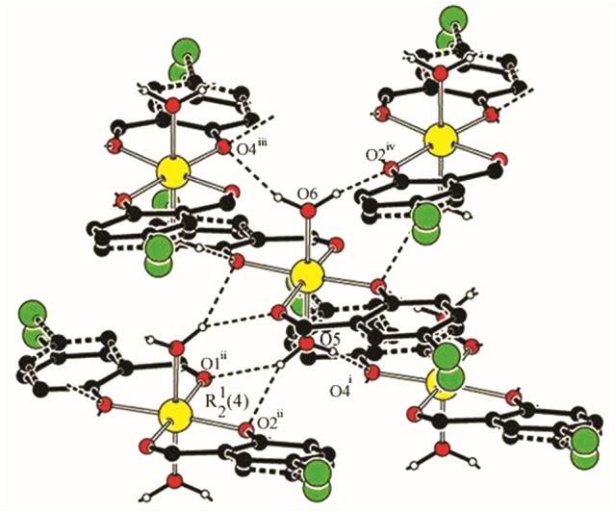

Fig. 2 — View of strong O – H...O hydrogen bonding.

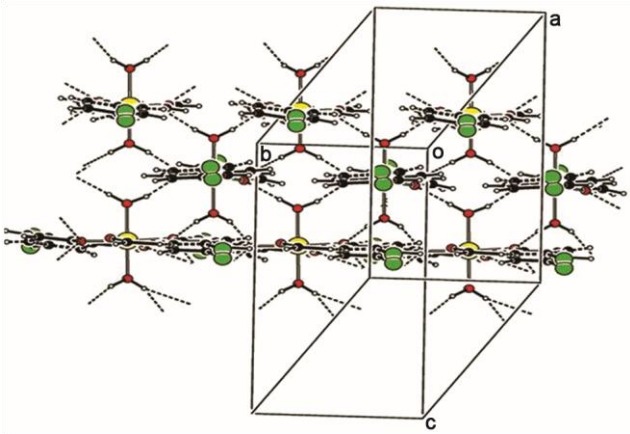

Fig. 3— Three dimensional overall packing interaction.

that have been arranged with d_{norm}(Fig. 4a), shape index (Fig. 4b), deformation density (Fig. 4c), curvedness (Fig. 4d) and disorder (Fig. 4e). The Hirshfeld surface is unique for the crystal structure of nickel complex and it measures volume (V_H), area (S_H), globularity (G) and asphericity (Ω). The term, globularity[21] is found to be less than unity for the crystal, which specifies that the molecular surface is more structured and is not a sphere. The asphericity[22] is a measure of anisotropy and is found to be 0.537. Shape index and curvedness can also be used to discover the characteristic packing modes and the ways in which the nearby molecules contact with one another. The red concave region on the surface is around the acceptor atom and a blue region is around the donor atom. In the 2D finger print plots (Fig. 5), two separate spikes appear for O..H/H..O intermolecular interactions (25.3%). The spike with O..H interaction corresponds to deprotonated oxygen donor of 5-bromo-2-hydroxy benzaldehyde with benzyl hydrogen and the spike with H..O interaction attributes to carbonyl oxygen and hydrogen in the same carbon. The upper spike corresponds to the H..O interaction (d_i=0.7Å, d_e=1.1Å) with 12.8% of Hirshfeld surface and lower spike being an O..H interaction (d_i=1.1Å, d_e=0.7Å) with 12.5% of the

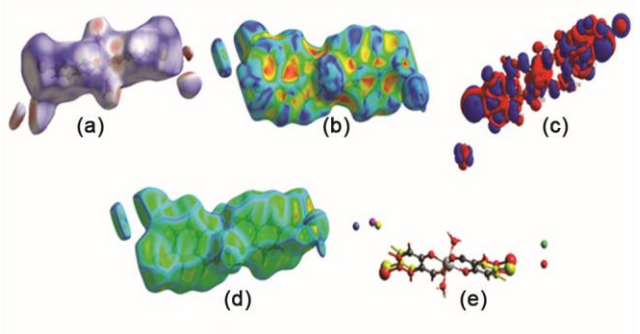

Fig. 4 — Hirshfeld surface mapped with (a) dnorm, (b) shape index, (c) deformation density, (d) curvednessand (e) disordered atoms of the molecule.

Table 3 — Hydrogen bonding interactions of the title compound (Å & °)

D—H...A	D—H	H...A	D...A	D—H...A(°)
O5—H5*A*...$O4^i$	0.91 (3)	1.88 (4)	2.766 (4)	164 (4)
O5—H5*B*...$O1^{ii}$	0.90 (3)	2.51 (4)	3.205 (4)	134 (5)
O5—H5*B*...$O2^{ii}$	0.90 (3)	2.12 (5)	2.943 (4)	151 (5)
O6—H6*A*...$O4^{iii}$	0.89 (3)	1.99 (4)	2.836 (4)	158 (4)
O6—H6*B*...$O2^{iv}$	0.89 (3)	1.90 (4)	2.741 (4)	157 (5)

Symmetry codes:
(i)−*x*, −*y*+1, −*z*; (ii) −*x*, −*y*, −*z*; (iii) −*x*, *y*−1/2,−*z*+1/2; (iv) −*x*, *y*+1/2, −*z*+1/2

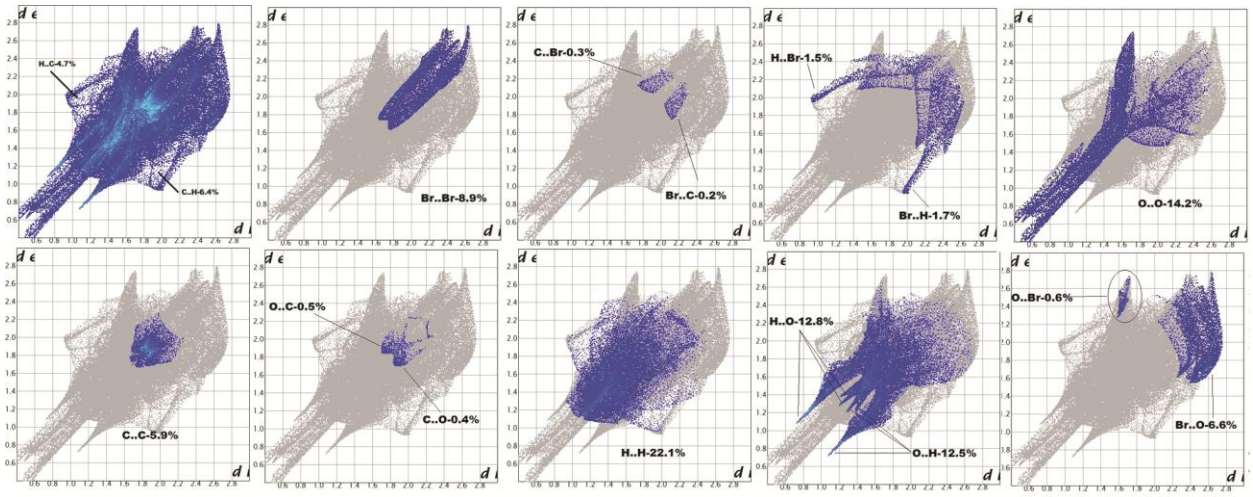

Fig. 5 — 2D fingerprint plots showing percentages of contacts contributed to the total Hirshfeld surface area of the molecule.

Hirshfeld surface of the molecule. The H…H interaction make up the majority of the Hirshfeld surface for the compound (22.1%). There is some C..C interactions also present which comprises 6% of the total Hirshfeld surface area of the molecule. The C..H interaction comprises approximately 11.1% of the surface. The C..O/O..C, Br/Br, H..Br/Br..H, O/O, C..Br/Br..C and O..Br/Br..O interactions are also observed and are 0.9%, 8.9%, 3.2%, 14.2%, 0.5% and 7.2%, respectively.

Molecular geometry

The optimized structure (Fig. 6), HOMO, LUMO and Mulliken charges and moleculer electrostatic potential were determined for the nickel complex. The bond lengths and bond angles are the geometrical parameters calculated by B3LYP/6-31G (d,p) methods and are compared with the same parameters obtained through XRD studies and are listed in the Table 1. A subtle difference in some bonding parameters has been observed. There is a little variation between the XRD and quantum chemically calculated values of the bond parameters. This may be due to the disorder of the molecule in solid state during crystallization.

The HOMO and LUMO orbital are elicited using DFT method and the energy differences between them delineate useful information regarding the chemical reactivity of the molecule. Molecular orbitals and their natural properties like energy, electron density aids to predict the most reactive position in the π-electron system and also explains several types of reactions in conjugated system. The HOMO-LUMO energy gap is specifying the kinetic stability of the complex[23]. The total energy, HOMO – 3, HOMO – 2,

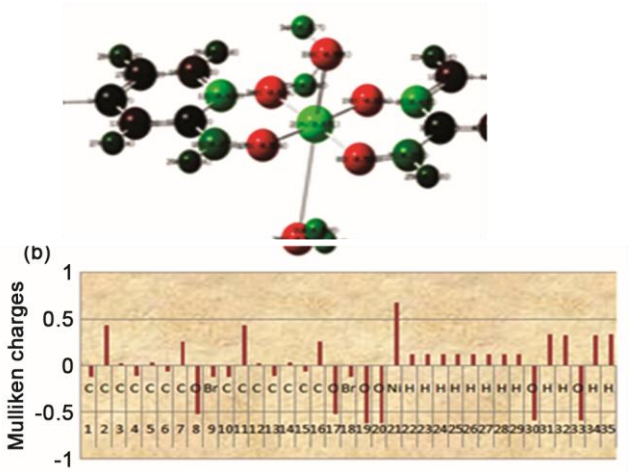

Fig. 6 — Optimized geometry of the complex.

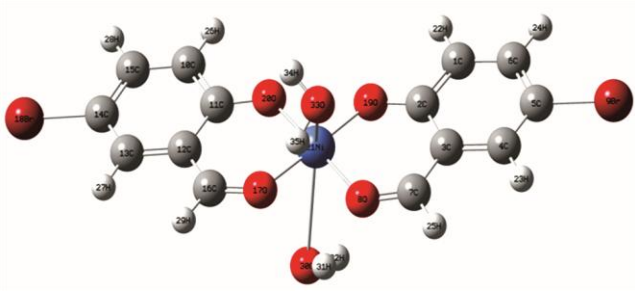

Fig. 7 — HOMO-LUMO energy gaps of the complex in various energy levels.

HOMO – 1, HOMO, LUMO, LUMO + 1, LUMO + 2 and LUMO + 3 energiesand the energy gaps are calculated and computed orbitals are displayed in the Fig. 7. The red and green colour indicates the positive and negative wave function values. The HOMO orbital is fully localised on all the atoms of the complex except bromine. The LUMO orbital is

localised on two salicylate moieties and bromine and water are left out. The energy gap between HOMO and LUMO is 0.0323a.u. The various chemical properties of the complex have been determined and listed in the Table 4. The chemical reactivity of the complex eventually helps to understand the biological activity of the drug molecule. The softness of the complex is high and the molecule is more polarisable. The Mullikan charges on the atoms in the molecule aids to outline the process of electronegativity equalization and charge transfer in chemical reactions. Mulliken charge distribution of the nickel complex has been represented in the Fig. 8. The most electropositive element in the complex is nickel. The carbon atoms C1, C4, C6, C10, C13 and C15 bear negative charges and acts as donor atoms and the remaining carbon atoms display positive charges. All the oxygen and bromine atoms show negative charge whereas all hydrogen atoms carry positive charge. There is a greater difference in the charge value of hydrogen attached to water and the bromo salicylate moiety. The graph (Fig. 9) displays the quantity of charge gained or lost by every atom on chelation and total charge bound with the fragment. The molecular electrostatic potential represents the charge distribution around the molecule in space and relates dipole moment, chemical reactivity and electro-negativity of the molecule. The electrostatic potential varies with atoms present and is represented by different colours. As the potential increases the colour varies from red < green < blue < pink < white. The MEP (Fig. 9) of the complex shows red colour around the oxygen atoms infers the more negativity over it. The blue colour is noted around the hydrogen atom of water molecule. Bromine atoms has green colour around it.

TD-DFT Calculation and electronic spectrum

To determine the existence of electronic transitions in the complex, TD-DFT calculation on the optimized geometry has been performed (Fig. 10a). A band at 7879 nm corresponds to HOMO → LUMO transition of 13% molecular contribution with oscillator strength of 0.0033. The wavelength of 2042 nm is due to transition from HOMO → LUMO + 2 with a major molecular contribution of 90% with f = 0.0128. The absorption band at 1347 nm is due to the excitation from HOMO → LUMO+1 with 41% of molecular contribution. Similarly at 633 nm, 608 nm and 586 nm electronic transitions are observed at various transitions and are listed in the Table 5. In the complex the experimental UV-DRS spectrum (Fig. 10b) reveals the wavelength of 622 nm is assigned to $^3A_{2g} \rightarrow {}^3T_{2g}(F)$ that matches with the simulated spectral bands which supports the octahedral geometry[24].

Table 4 — Chemical reactivity descriptors of the title compound

Parameters (a.u.)	*Values*
Ionisation potential (I)	0.13067
Electron affinity (A)	0.0983
Global hardness (η)	0.01619
Chemical potential (μ)	0.11449
Global electrophilicity (ω)	0.4049
Softness (S)	61.7856

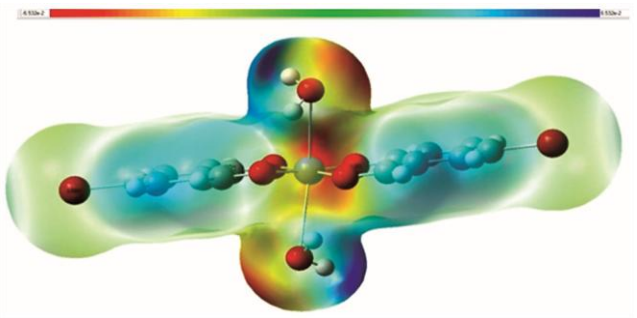

Fig. 8 — Pictorial representation of Mulliken charges of the complex.

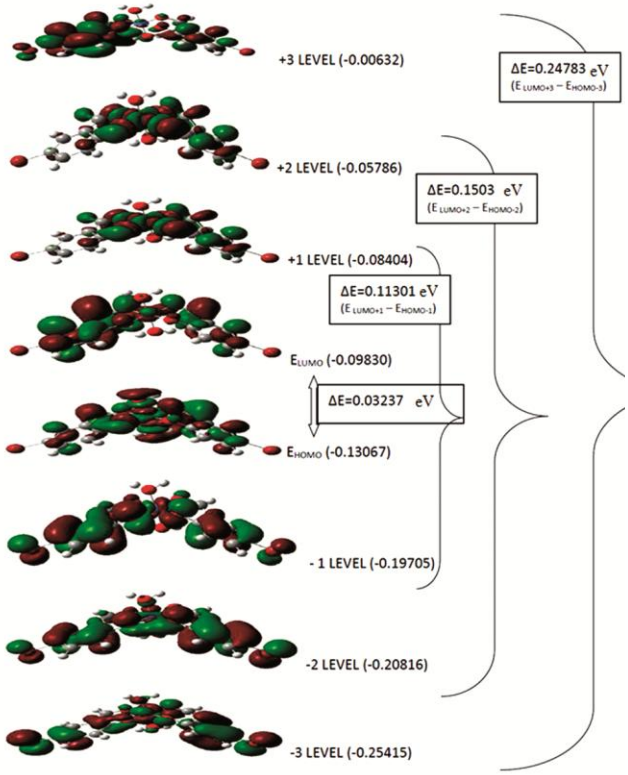

Fig. 9 — Molecular electrostatic potential of the complex.

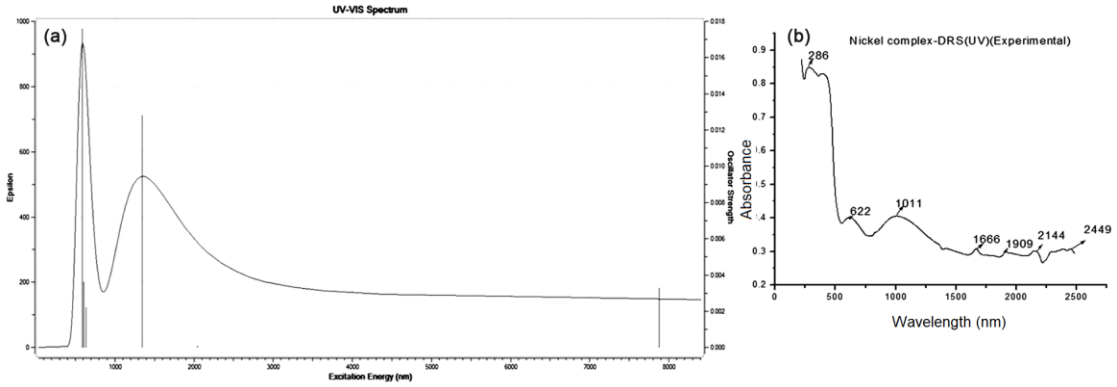

Fig. 10 — UV spectra of the title compound: (a) Theoretical and (b) Experimental.

Table 5 — TD-DFT calculation for singlet-singlet electronic transition of the title compound

Key Excitations (Molecular Contribution)	E (eV)	λ (nm)	Osc. Strength (f)	λ_{expt} (nm)
HOMO→LUMO (13%)	0.1574	7879	0.0033	-
HOMO→LUMO+2 (90%)	0.0607	2042	0.0128	2144
HOMO→LUMO+1 (41%)	0.9205	1347	0.0128	1666
HOMO-1→LUMO+1 (59%)	1.9568	633	0.0022	-
HOMO-1→LUMO (84%)	2.0393	608	0.0036	622
HOMO-2→LUMO+1 (27%)	2.1164	586	0.0176	-

Conclusions

In this paper, we have synthesized diaquabis (5-bromo-1-formyl phenolato-k^2 O,O')nickel (II) monohydrate and its structure has been established through single crystal X-ray diffraction studies in detail. The molecule is found to be a neutral mononuclear nickel complex and adopts octahedral geometry. The monoclinic, $P2_1/c$ lattice is stabilized by relatively strong hydrogen bonds. The Hirshfeld surface of the complex has been mapped with d_{norm}, shape index, deformation density and curvedness. The DFT calculations and experimental XRD results of the title compound have been compared with each other, which show excellent unification with each other. The Mulliken charges, HOMO and LUMO calculations were also reported for the title compound. The UV – visible NIR spectrum of the complex is compared with simulated UV spectrum of the complex through TD-DFT calculations. The simulated spectrum comparatively matches well with the experimentally obtained UV spectrum.

Supplementary Data

CCDC-945220 contains the supplementary crystallographic data for this paper. These data can be obtained free of charge at www.ccdc.cam.ac.uk/ consts/retrieving.html (or from the Cambridge Crystallographic data centre (CCDC), 12, Union Road, Cambridge CB2 IE2, UK, Fax: C44 (0)1223-336033; email-deposit@ccdc.cam.ac.uk).

Acknowledgement

Authors would like to acknowledge SAIF, IIT Madras for X-ray crystallographic analysis. The authors extend their sincere thanks to The Secretary, Principal and Faculty members of Chemistry, SeethalakshmiRamaswami College, Tiruchirappalli, Tamil Nadu for providing laboratory facilities and support.

References

1 Zhao B, Cheng P, Dai Y, Cheng C, Liao D Z, Yan S P, Jiang Z H & Wang G L, *Angew Chem Int*,42 (2003) 934.
2 Ruben M, Rojo J, Romero-Salguero F J, Uppadine L H & Lehn J M, *AngewChemInt*,43 (2004) 3644.
3 Gao X M, Li D S, Wang J J, Fu F, Wu Y P, Hu H M & Wang J M, *CrystEngComm*,5 (2008) 479.
4 Yang G P, Wang Y Y, Liu P, Fu A Y, Zhang Y N, Jin J C & Shi Q N, *Cryst Growth Des*,10 (2010) 1443.
5 Yang G P, Zhou J H, Wang Y Y, Liu P, Shi C C, Fu A Y & Shi Q Z, *CrystEngCommun*, 13 (2011) 33.
6 Yang G P, Wang Y Y, Zhang W H, Fu A Y, Liu R T, Lermontovaab E K & Shi Q Z, *CrystEngCommun*, 12 (2010) 1509.
7 Maurya R C, Chourasia J, Rajak D, Malik B A, Mir J M, Jain N & Batalia S, *Arab J Chem*, 9 (2016) s1084.
8 Onada A, Yamada Y, Doi M, Okamura T & Ueyama N, *Inorg. Chem*,4 (2001) 516.
9 Ma J F, Yang J & Liu J F, *Acta Crystallogr Sec E*,59 (2003a) m478.
10 Ma J F, Yang J & Liu J F, *Acta Crystallogr Sec E*,59 (2003b) m481.
11 Ma J F, Yang, J, & Liu J F, *ActaCrystallogr Sec E*, 59 (2003c) m483.
12 Ma J F, Yang J & Liu J F, *Acta Crystallogr Sec E*,59 (2003d) m485.
13 Ma J F, Yang J & Liu J F, *Acta Crystallogr Sec E*,59 (2003e) m487.
14 Rama I & Selvameena R, *J Chem. Sci*, 127 (2015)671.
15 Bruker (2001) SMART, SAINT and SADABS Bruker AXS Inc, Madison, Wisconsin, USA.

16 Sheldrick GM (1997) SHELXS-97 and SHELXL-97, University of Gottingen, Germany.
17 Spek A L, *J Appl Crystallogr*, 36 (2003) 7.
18 Frisch M J, Trucks G W, Schlegel H B, Scuseria G E, Robb M A,Cheeseman J R, Montgomery Jr J A, Vreven T, KudinK N, Burant J C, Millam J M, Iyengar S S, Tomasi J, Barone V, Mennucci B, Cossi M, Scalmani G, Rega N, Petersson G A, Nakatsuji H, Hada M, Ehara M, Toyota K, Fukuda R, Hasegawa J, Ishida M, Nakajima T, Honda Y, Kitao O, Nakai H, Klene M, Li X, Knox J E, Hratchian H P, Cross J B, Adamo C, Jaramillo J, Gomperts R, Stratmann R E, Yazyev O, AustinA J, Cammi R, Pomelli C, Ochterski J W, Ayala P Y, Morokuma K, Voth G A, Salvador P, Dannenberg J J, Zakrzewski V G, Dapprich S, Daniels A D, Strain M C, Farkas O,Malick D K, Rabuck A D, RaghavachariK, Foresman J B, Ortiz J V, Cui Q, Baboul A G, Clifford S, Cioslowski J, Stefanov B B, Liu G, Liashenko A, Piskorz P, Komaromi I, Martin R L, Fox D J, Keith T, Al-Laham M A, Peng C Y, Nanayakkara A, Challacombe M, Gill P M W, Johnson B, Chen W, Wong M W, Gonzalez C & Pople J A, (2004) "Gaussian 03",Gaussian, Inc., Wallingford CT.
19 Patel R N, *Indian J Chem*, 48A (2009)173.
20 Wolff S K, Grimwood D J, McKinnon J J, Turner M J, Jayatilaka D & Spackman M A, (2012) University of Western Australia, Crystal Explorer (Version 3.1).
21 Meyer A Y, *Chem Soc* Rev, 15 (1986) 449.
22 Rudnick J & Gaspari G, *J.Phys A Math. Gen Phys*, 19 (1986) L191.
23 Aditya Prasad A, Muthu K, Meenatchi V, Rajasekar M, Agilandeshwari R, Meena K, VijilaManonmoni J & Meenakshisundaram S P, *Spectrochim. Acta A*, 140 (2015) 311.
24 Veera Reddy K, *Symmetry and Spectroscopy of Molecules*, (New Age International, New Delhi, India) 2017.